


MAXIMUM INFORMATION EXTRACTION FROM NOISY DATA VIA SHANNON ENTROPY MINIMIZATION

PREPRINT

 **Matteo Becchi**

Department of Applied Science and Technology
Politecnico di Torino
Corso Duca degli Abruzzi, 24, 10129 Torino

 **Giovanni M. Pavan***

Department of Applied Science and Technology
Politecnico di Torino
Corso Duca degli Abruzzi, 24, 10129 Torino

April 21, 2025

ABSTRACT

Granting maximum information extraction in the analysis of noisy data is non-trivial. We introduce a general, data-driven approach that employs Shannon entropy as a transferable metric to quantify the maximum information extractable from noisy data via their clustering into statistically-relevant micro-domains. We demonstrate the method's efficiency by analyzing, as a representative example, time-series data extracted from molecular dynamics simulations of water and ice coexisting at the solid/liquid transition temperature. The method allows quantifying the information contained in the data distributions (time-independent component) and the additional information gain attainable by analyzing data as time-series (i.e., accounting for the information contained in data time-correlations). The approach is also highly effective for high-dimensional datasets, providing clear demonstrations of how considering components/data that may be little informative but noisy may be not only useless but even detrimental to maximum information extraction. This provides a general and robust parameter-free approach and quantitative metrics for data-analysis, and for the study of any type of system from its data.

Keywords Information gain · Shannon entropy · Data clustering · Time-series · Data science

Scientific data analysis often requires critical methodological choices – such as the selection of observables, resolution, and analysis parameters – that significantly influence both the extraction and interpretation of physical information [1]–[3]. These choices are frequently guided by heuristic conventions, prior experience, or implicit assumptions, which can introduce bias and compromise the robustness and reliability of the results [4], [5]. Here we present a robust, data-driven approach based on information theory to optimize methodological choices, thereby maximizing the extraction of relevant information through clustering data into statistically relevant micro-domains. This method, referred to as “Maximum Information Extraction” (MInE), is versatile and applicable to both mono- and high-dimensional datasets. Specifically, we demonstrate its effectiveness in extracting information from noisy time-series data.

Various algorithms have been developed to optimize specific analysis parameters [6], [7]. While effective, these methods typically focus on isolated steps in data acquisition or processing – such as feature selection [8]–[11], clustering [12], [13], or coarse-graining [14], [15] – making it difficult to assess and compare the impact of different choices using a unified, transferable metric. In contrast, MInE employs a Shannon entropy-based metric to quantify the information gain (i.e., entropy decrease) achieved through clustering across various cases and setups, providing a principled criterion for identifying the optimal methodological choices and analysis setup for maximizing information extraction. In the case of noisy time-series data, detecting statistically relevant micro-domains through single point clustering depends on the resolution Δt used to segment and analyze the data [16]–[18]. Among the available algorithms for single point time-series analysis [19], we use onion clustering [17], an unsupervised method that identifies all statistically relevant micro-domains (including hidden ones) that can be resolved in a

*Corresponding author: giovanni.pavan@polito.it

time-series of length τ as a function of Δt , as well as the fraction of unclassifiable data due to insufficient resolution.

Note that the MInE workflow makes this method different from entropy-minimization based clustering algorithms [20]. Shannon entropy minimization is not used in MInE to guide the clustering itself, but it is rather applied *a posteriori* to evaluate the effectiveness of the methodological choices for the clustering and to quantify the information attainable from it. To this regard, while onion clustering is particularly well suited to this end, and is thus chosen as a basis for the demonstrations presented herein, the MInE method is general and can in principle be applied in combination with any clustering technique.

By using Shannon entropy as a transferable metric, MInE compares the information extractable as a function of the micro-clusters resolvable (and the fraction of unclassifiable data) at various Δt . The optimal resolution [16] and best analysis setup for maximum information extraction are identified as those that minimize Shannon entropy. We demonstrate the effectiveness of MInE through two case studies. First, we compare the information extractable from mono-variate time-series data—obtained using different descriptors [21]–[23] from Molecular Dynamics (MD) trajectories of water and ice phases coexisting at the melting temperature—as a function of resolution and/or descriptor choice. Second, in a model Langevin dynamics on a bi-dimensional energy landscape, we show how MInE can assess how information extraction is influenced by the interplay between the number of dimensions considered and the impact of noisy data and frustrated information phenomena [18] in high-dimensional, multi-variate analyses. These case studies highlight MInE as a general method for optimizing data analysis and maximizing the knowledge attainable from data.

The Shannon entropy [24] of an observable x , which takes values in a set \mathcal{X} with probability distribution $p(x)$, is defined as:

$$H(x) = - \sum_{x \in \mathcal{X}} p(x) \log_2 p(x) \quad (1)$$

This quantity measures the uncertainty in x , with higher entropy indicating a broader distribution and lower entropy corresponding to more sharply concentrated distributions. For a dataset clustered into K clusters with probability distributions $p_k(x)$, the Shannon entropy of the clustered system is:

$$H_{\text{clust}}(x) = \sum_{k=1}^K f_k H_k \quad (2)$$

where f_k is the fraction of data points in cluster k , and H_k is the Shannon entropy of the data within that cluster. By convexity, clustering never increases entropy, and the corresponding information gain is thus defined as:

$$\Delta H = H(x) - H_{\text{clust}}(x) \geq 0 \quad (3)$$

This quantity measures the reduction in uncertainty achieved *via* data clustering [25]. Normalizing by the initial entropy, $\Delta H/H(x)$ provides a dimensionless metric of how effectively clustering extracts information from the data by reducing entropy. A trivial clustering – where all points belong to a single cluster, or are assigned randomly – yields $\Delta H \sim 0$, indicating little to no information gain. In contrast, an effective clustering maximizes ΔH , successfully extracting meaningful structure from the data.

In our implementation, entropy H is estimated from the histograms of the dataset before and after clustering, using a consistent binning scheme to ensure comparability. To facilitate interpretation, all entropy values (which following Eq. 1 are measured in bits) in this work are normalized with respect to the maximum possible entropy value $\log_2 n_b$ bit, providing an adimensional quantity (see Supplemental Material for complete details on the method). Note that, while here Shannon entropy is our primary measure for building our method, alternative information-theory based metrics (such as, when dealing with time-series, e.g., Approximate Entropy [26] or Sample Entropy [27], [28]) can also be employed within the same framework.

As a first example, we tested the MInE framework to analyze MD simulation trajectories of 2048 TIP4P/ICE [29] molecules coexisting in dynamic equilibrium between solid and liquid phases at the melting temperature (Fig. 1a). After equilibration, we performed a $\tau = 50$ ns production run under *NPT* conditions, sampling trajectories every 0.04 ns (complete simulation details are provided in the Supplemental Material). We used various single-particle descriptors to extract univariate time-series data from the MD trajectories, each capturing distinct structural and/or dynamical features of the system, with its own signal-to-noise ratio [30], [31]. For example, Figs. 1 and 2 show results obtained using the Smooth Overlap of Atomic Positions (SOAP) [21], which provides a rotationally invariant, high-dimensional representation of the local molecular density around each molecule (Fig. 1b). The SOAP power spectrum offers a fingerprint of the spatial arrangement of neighboring molecules within a sphere of radius r_c around each molecule.

In the following, we show as a representative example the results obtained by analyzing denoised [32] time-series data of the first principal component (PC1) of the SOAP vectors, which has been recently shown to be an informative descriptor for such systems [18], [31] (complete description for the SOAP analysis are provided in the Supplemental Material). Data obtained with other descriptors [23] and/or by reducing the dimensionality of the SOAP spectra with other methods (e.g., *via* Time-lagged Independent Component Analysis [33], [34]) are reported in the Supplementary Material.

Fig. 1c shows the SOAP PC1 time-series data for all molecules along the trajectory (in black), with one

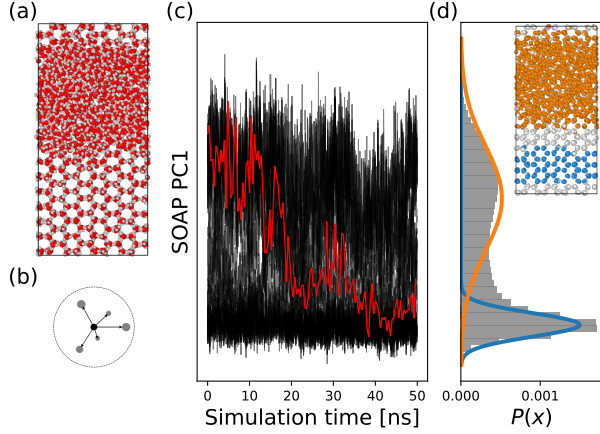


Figure 1: (a) Snapshot of the water/ice atomistic model system used as a case study. (b) Schematic of the SOAP descriptor, which provides a high-dimensional representation of the density, order/disorder, and symmetry of the arrangement of neighboring molecules around each molecule. (c) Denoised [32] PC1 SOAP time-series [18], [31] for the 2048 molecules as a function of simulation time. In red: the signal of a representative molecule undergoing a water-to-ice transition. (d) Probability distribution $P(x)$ of the SOAP PC1 signals (gray). Two main clusters, corresponding to the liquid and ice phases (inset), are identified by the two maxima in $P(x)$ (orange and blue Gaussian fits). These clusters are readily detected using pattern recognition methods (see Supplemental Material for details).

molecule undergoing an ice-to-water transition highlighted in red. The probability distribution $P(x)$ of the entire SOAP PC1 dataset is shown in Fig. 1d (gray). The two prominent density peaks in $P(x)$ allow typical clustering methods to readily identify two main clusters in the data. These clusters, represented by the orange and blue Gaussian curves centered on the $P(x)$ peaks in Fig. 1d, correspond to the liquid and solid phases, as shown in the snapshot inset with matching color coding.

However, additional information is embedded in the data, particularly in their temporal correlations [17]. This is evident from the results obtained by onion clustering at smaller Δt (i.e., increasing the temporal resolution). Complete onion clustering results are shown in Fig. S1, showing that the number of resolvable clusters is maximized in the resolution interval $2 \text{ ns} \lesssim \Delta t \lesssim 20 \text{ ns}$. Within this range, the method identifies three statistically distinct clusters corresponding to the ice and water phases, and the ice/water interface (see Fig.S1).

Note that results such as the number and quality of detected clusters, as well as the fraction of unclassified data, are descriptor-dependent. Each descriptor is characterized by its own signal-to-noise ratio, and its feature space is defined by metrics that differ from those of other descriptors. As a result, it is not trivial to unambiguously infer, for example, whether the information captured by the SOAP

PC1 descriptor represents the maximum extractable information, or how one descriptor compares to another. MInE overcomes this limitation by using entropy as a transferable metric. It exploits Shannon entropy minimization to assess the maximum information that can be extracted from the data following clustering, as defined by Eq. 3.

Figure 2 shows the information I attainable from the data before and after clustering. By normalizing the Shannon entropy between 0 and 1, the relationship $I = 1 - H$ holds. Consequently, the information that can be effectively extracted from the data ranges from $0 \leq I \leq 1$. In the hypothetical case where all information content is resolved, $I = 1$, while $I = 0$ corresponds to the case where the data are completely random, containing no structure, and no statistically relevant information can be extracted.

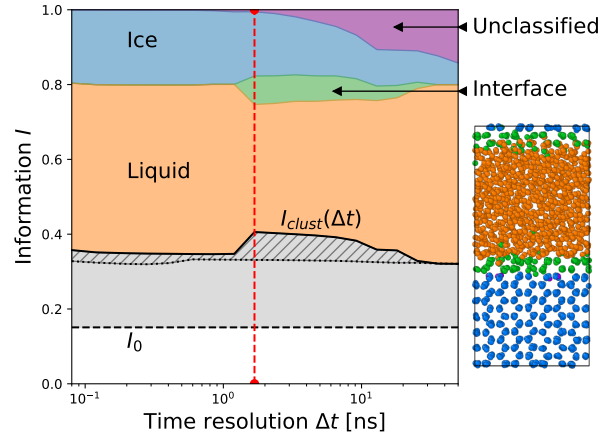


Figure 2: Information gain from onion clustering as a function of the time resolution Δt used in the analysis. The horizontal dashed line represents the information content of the raw data distribution ($I_0 = 0.151$). The solid black curve labeled I_{clust} represents the information retained after clustering, which varies with Δt . I_{clust} reaches a maximum at $\Delta t \sim 2 \text{ ns}$ (vertical red dashed line), indicating the optimal time resolution for extracting information from the SOAP PC1 time-series. The area shaded in gray corresponds to the increase in the information content of the data achieved through clustering. The dotted line reports the information gain through clustering on the dataset where the frames have been randomly reshuffled, and the area with diagonal hatching is the increment in information gain due to leveraging the time correlations. A snapshot of the simulation, colored according to onion clustering at this resolution, reveals bulk ice and liquid water in blue and orange, respectively, with the solid-liquid interface in green. A small fraction of unclassifiable data points appears as sparse molecules colored in purple. The width of the colored regions in the plot corresponds to the weighted Shannon entropy $f_k H_k$ of each environment, illustrating how entropy varies with Δt (colors correspond to those in the simulation snapshot).

The information contained in the data probability distribution $P(x)$ (prior to clustering) can be quantified by its Shannon entropy, H_0 (calculated *via* Eq. 1), as $I_0 = 1 - H_0 \sim 0.151$ (black horizontal dashed line in Fig. 2). Since this value depends solely on the data distribution, it is independent of the time resolution Δt used in the subsequent clustering analysis. In contrast, the information content after clustering is given by $I_{\text{clust}}(\Delta t) = 1 - H_{\text{clust}}(\Delta t)$, represented by the solid black curve in Fig. 2. The gray-shaded area between these two curves represents the total information gain extractable, in this case, by onion clustering. Shannon entropy minimization is achieved at $\Delta t^* = 1.8$ ns (vertical red dashed line), where the maximum information $I_{\text{max}} = I_{\text{clust}}(\Delta t^*) \sim 0.41$ is attained. At all resolutions, the sum of the resolved information I and the residual entropy H remains constant (by definition). Above the solid black line in Fig. 2, the weighted Shannon entropy of the different resolved environments (micro-clusters), $f_k H_k$, is shown for each value of Δt . As seen in Fig. 2, within the range of Δt where the ice/water interface (green area) is resolved as a distinct micro-cluster, the information I_{clust} is maximized when the fraction of unclassified data points (in violet) is minimized.

From an information-theoretic perspective, the disappearance of the interface cluster (green) leads to an increase in the residual entropy $f_k H_k$ of the remaining clusters (Fig. 2). Conversely, when the interface is detected, the total entropy in Eq. 2 decreases, despite the introduction of an additional term. This is because the reduction in $f_k H_k$ for the ice and liquid phases more than compensate for the added entropy contribution of the interface. Physically, the optimal range $2 \text{ ns} \lesssim \Delta t \lesssim 20 \text{ ns}$ provides the best balance between resolution and noise, enabling the identification of the ice/water interface, which has a characteristic residence time of ~ 10 ns [35]. At lower time resolutions ($\Delta t \geq 20$ ns), an increasing fraction of data points remains unclassified, resulting in a raise in the residual entropy H_{clust} and a corresponding decrease in the information gain (gray area in Fig. 2). On the other hand, at higher resolutions ($\Delta t \leq 1$ ns), the interface can no longer be resolved as a distinct environment. This occurs because excessively fine temporal segmentation emphasizes short-time molecular vibrations – interpreted as noise – at the expense of capturing the physically meaningful transitions between phases [18].

To estimate the contribution of time correlations to the total information I_{clust} , we repeated the Onion clustering analysis after randomly reshuffling the time-series frames. This procedure preserves the data probability distribution $P(x)$, while effectively removing temporal correlations, thereby eliminating any information that could be extracted from them. We performed this reshuffling ten times and computed the average values of I_{clust} as a function of Δt ; the variance in the estimation was consistently below 0.1% for all Δt . The results are shown in Fig. 2 as a dotted curve. Notably, this curve is nearly horizontal, indicating that – once time correlations are removed – the extractable information becomes largely independent of the resolu-

tion Δt . Furthermore, the value of I_{clust} obtained from the reshuffled data closely matches that obtained from the original time-series when analyzed at the lowest possible resolution ($\Delta t = \tau = 50$ ns). In Fig. 2, the difference between the I_0 baseline (dashed line) and the reshuffled I_{clust} (dotted line) represents the information gain achievable via clustering under a purely ergodic approximation – that is, neglecting time correlations. Finally, the difference between this dotted I_{clust} curve and the solid black $I_{\text{clust}}(\Delta t)$ curve (corresponding to the original time-ordered series) quantifies the additional information that is uniquely encoded in the temporal correlations – highlighted by the diagonally hatched gray area in Fig. 2.

Beyond identifying the optimal resolution for maximum information extraction from a dataset through clustering, MInE also enables a direct comparison of the effectiveness of different descriptors in extracting relevant information from the same trajectory. This comparison is made possible by the transferable nature of the Shannon entropy-based metric. As shown in Fig. S2 in the Supplemental Material, we applied MInE to time-series derived from different descriptors, as well as from alternative dimensionality-reduction techniques applied to SOAP spectra [33], [34]. These analyses reveal, for this specific system, the existence of descriptors that are better suited for maximizing information extraction. For instance, the LENS descriptor [23] achieves a higher information gain across a broader range of resolutions compared to others, demonstrating its ability to capture the relevant physical dynamics encoded in the molecular trajectories.

MInE can also be applied to high-dimensional datasets and multivariate time-series. When using multivariate descriptors, quantifying information becomes particularly relevant in tasks such as feature selection and dimensionality reduction. These approaches aim at reduce data complexity but often involve trade-offs, as decreasing the number of variables can lead to information loss. To explore this, we tested the MInE framework on a simple multivariate model dataset. Specifically, we simulated the Langevin dynamics of 100 particles in two distinct bi-dimensional potential energy landscapes: one with four minima (A to D), requiring both (x, y) coordinates for proper identification, and another with only two minima (A and B), distinguishable using the y coordinate alone. In both cases, all minima are subject to identical Gaussian noise (Fig. 3a). We then applied the same MInE procedure as described above to four different datasets, obtained by analyzing both systems using either the full (x, y) coordinates or only the y coordinate through onion clustering (see Supplemental Material for full details on these test cases).

The information gain obtained after clustering for these model systems is shown in Fig. 3b. For the system with four energy minima (Fig. 3b, left), using both (x, y) coordinates all four minima to be identified. In contrast, using only the y coordinate does not distinguish between A and C or between B and D, which collapse into two degenerate (and doubly-populated) A+C and B+D states.

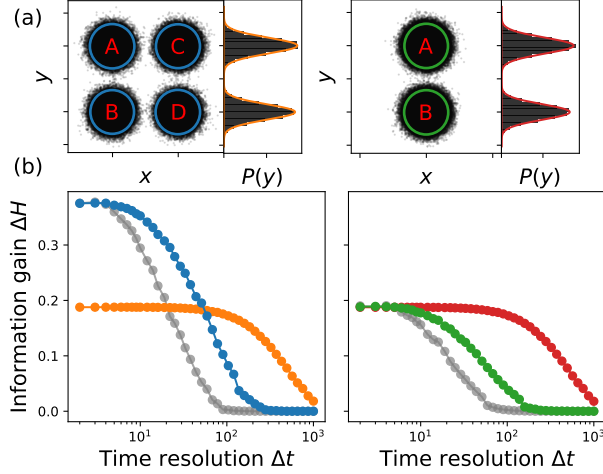


Figure 3: (a) From left to right, the trajectories of 100 particles in a bi-dimensional energy landscape with 4 and 2 minima respectively, and the probability distribution of the y coordinate $P(y)$. The clusters identified by onion clustering in the two systems, using the full (x, y) trajectories or only the y coordinate, are shown in blue, orange, green and red respectively. (b) The information gain ΔH through onion clustering as a function of the time resolution Δt (measured in simulation time-steps), on the two datasets for each system (left and right respectively). The colors match the ones of panel (a). In gray, the case when using also a z coordinate containing only Gaussian noise.

Comparing the blue and orange curves highlights that the maximum attainable information gain (reached in this system for $\Delta t < 5$ frames) is twice as high when performing a bi-dimensional analysis (blue) compared to a mono-dimensional one (orange). For the system with just two minima (Fig. 3b, right), the maximum attainable information gain is the same whether using both (x, y) or just the y coordinate (green vs. red curves): in this case, both minima are correctly identified regardless of dimensionality, making the second variable unnecessary. Importantly, the maximum information gain is identical in the orange curve (mono-dimensional analysis of the four-minima system) and the red and green curves (two-minima system), despite representing different systems and analyses. This demonstrates how Shannon entropy within the MInE framework serves as an objective, transferable, and quantitative metric for assessing and comparing the extractable information across datasets and analysis strategies.

Interestingly, in both systems, the information gain (and thus clustering performance) decreases more rapidly with increasing Δt in the bi-dimensional analyses (blue and green curves) compared to the mono-dimensional ones (orange and red). In the four-minima system, one initial hypothesis attributed this behavior to the “apparent” longer residence times of particles in the degenerate A+C and B+D states identified by the mono-dimensional analysis, compared to the shorter residence times in the individ-

ual A, B, C, and D states resolved by the bi-dimensional one. However, this explanation does not hold for the two-minima system (Fig. 3b, right), where both A and B states are correctly identified in both types of analyses – yet the same faster decrease in information gain with increasing Δt is observed in the bi-dimensional case. These findings for the two-minima case point instead to the role of noise-addition phenomena that can affect high-dimensional analyses: specifically, even though the x component in this case does not provide relevant information, it still introduces noise [18]. In higher-dimensional spaces, clustering algorithms tend to leave a larger fraction of data points unclassified [18], [36], as also shown in Fig. S3 of the Supplemental Material. As discussed elsewhere [18], these results underscore how including additional (noisy) dimensions may be not only unhelpful, but actually detrimental to the effectiveness of high-dimensional analyses.

To further validate these effects, we performed an additional test in both systems by introducing a third dimension z , which – like x in the previous test – does not carry any meaningful information but only contributes Gaussian noise (i.e., all minima are characterized by identical, uncorrelated noise in all directions). The gray curves in Figs. 3b,c show that while the maximum attainable information remains unchanged compared to the lower-dimensional cases, the range of Δt values over which this information is effectively extractable becomes further reduced. This confirms that adding increasingly noisy components hinders the extraction of meaningful information, particularly that embedded in the time-correlations of the data. These findings reflect a manifestation of the so-called “curse of dimensionality” [37], [38], highlighting that in clustering analyses there exists a threshold beyond which the inclusion of additional dimensions shifts from enriching the information content to merely introducing noise. MInE proves particularly valuable in this context, as it enables probing and quantifying these effects in a rigorous and interpretable way.

We underline that, while the results above focus on time-series data – where temporal correlations play a key role – the MInE approach is general and applicable to other types of datasets as well. For example, in the case of static data distributions (or in situations where time correlations are irrelevant or difficult to resolve), the I_{clust} becomes independent of the Δt . In such contexts, MInE can be thus used to identify, e.g., the most effective clustering method, or parameter set (descriptor(s)) that allows minimizing Shannon entropy and maximizing information extraction from the data distributions.

In conclusion, we have introduced a novel data-driven framework based on information gain to optimize data analysis and achieve maximum information extraction (MInE) through clustering, applicable to any type of dataset. By employing Shannon entropy as a transferable and objective metric, MInE enables a clear and quantitative assessment of the amount of information that can be effectively resolved in diverse datasets – depending, for example, on

the resolution, clustering method, or descriptor adopted in the analysis. Given the central role of data clustering and feature selection in scientific discovery, we anticipate that MInE – along with its use of information gain as an objective criterion for evaluating and comparing analyses – will prove valuable across a broad range of fields, including materials science, complex systems, biology, and data science at large.

Data availability

All the code and data necessary to reproduce the analysis of this work are available on a Zenodo repository at [39].

Acknowledgments

The authors thank Chiara Lionello for the insightful discussions. G.M.P. acknowledges the support received by the European Research Council (ERC) under the Horizon 2020 research and innovation program (grant agreement no. 818776 - DYNAPOL).

References

- [1] J. Liepe, P. Kirk, S. Filippi, T. Toni, C. P. Barnes, and M. P. Stumpf, “A framework for parameter estimation and model selection from experimental data in systems biology using approximate bayesian computation,” *Nature protocols*, vol. 9, no. 2, pp. 439–456, 2014. DOI: 10.1038/nprot.2014.025.
- [2] G. Bonaccorso, *Machine Learning Algorithms: Popular algorithms for data science and machine learning*. Packt Publishing Ltd, 2018.
- [3] J. Ding, V. Tarokh, and Y. Yang, “Model selection techniques: An overview,” *IEEE Signal Processing Magazine*, vol. 35, no. 6, pp. 16–34, 2018. DOI: 10.1109/MSP.2018.2867638.
- [4] T. E. Sweeney, A. C. Chen, and O. Gevaert, “Combined mapping of multiple clustering algorithms (communal): A robust method for selection of cluster number, k,” *Scientific reports*, vol. 5, no. 1, p. 16971, 2015. DOI: 10.1038/srep16971.
- [5] M. C. Thrun, “Distance-based clustering challenges for unbiased benchmarking studies,” *Scientific reports*, vol. 11, no. 1, p. 18988, 2021. DOI: 10.1038/s41598-021-98126-1.
- [6] H. Kohjitani, S. Koda, Y. Himeno, *et al.*, “Gradient-based parameter optimization method to determine membrane ionic current composition in human induced pluripotent stem cell-derived cardiomyocytes,” *Scientific Reports*, vol. 12, no. 1, p. 19110, 2022. DOI: 10.1038/s41598-022-23398-0.
- [7] B. Bischl, M. Binder, M. Lang, *et al.*, “Hyperparameter optimization: Foundations, algorithms, best practices, and open challenges,” *Wiley Interdisciplinary Reviews: Data Mining and Knowledge Discovery*, vol. 13, no. 2, e1484, 2023. DOI: 10.1002/widm.1484.
- [8] W. Siedlecki and J. Sklansky, “On automatic feature selection,” *International Journal of Pattern Recognition and Artificial Intelligence*, vol. 2, no. 02, pp. 197–220, 1988. DOI: 10.1142/S0218001488000145.
- [9] A. Arauzo-Azofra, J. M. Benitez, and J. L. Castro, “Consistency measures for feature selection,” *Journal of Intelligent Information Systems*, vol. 30, pp. 273–292, 2008. DOI: 10.1007/s10844-007-0037-0.
- [10] A. Glielmo, C. Zeni, B. Cheng, G. Csányi, and A. Laio, “Ranking the information content of distance measures,” *PNAS nexus*, vol. 1, no. 2, pgac039, 2022. DOI: 10.1093/pnasnexus/pgac039.
- [11] R. Wild, E. Sozio, R. G. Margiotto, *et al.*, “Maximally informative feature selection using information imbalance: Application to covid-19 severity prediction,” *Scientific Reports*, vol. 14, no. 1, p. 10744, 2024. DOI: 10.1038/s41598-024-61334-6.
- [12] M. Sugiyama, M. Yamada, M. Kimura, and H. Hachiya, “On information-maximization clustering: Tuning parameter selection and analytic solution,” in *Proceedings of the 28th International Conference on Machine Learning (ICML-11)*, 2011, pp. 65–72.
- [13] E. Aldana-Bobadilla and A. Kuri-Morales, “A clustering method based on the maximum entropy principle,” *Entropy*, vol. 17, no. 1, pp. 151–180, 2015. DOI: 10.3390/e17010151.
- [14] P. Gkeka, G. Stoltz, A. Barati Farimani, *et al.*, “Machine learning force fields and coarse-grained variables in molecular dynamics: Application to materials and biological systems,” *Journal of chemical theory and computation*, vol. 16, no. 8, pp. 4757–4775, 2020. DOI: 10.1021/acs.jctc.0c00355.
- [15] S. Y. Joshi and S. A. Deshmukh, “A review of advancements in coarse-grained molecular dynamics simulations,” *Molecular Simulation*, vol. 47, no. 10-11, pp. 786–803, 2021. DOI: 10.1080/08927022.2020.1828583.
- [16] D. Doria, S. Martino, M. Becchi, and G. M. Pavan, *Data-driven assessment of optimal spatiotemporal resolutions for information extraction in noisy time series data*, 2025. arXiv: 2412.13741 [physics.data-an].
- [17] M. Becchi, F. Fantolino, and G. M. Pavan, “Layer-by-layer unsupervised clustering of statistically relevant fluctuations in noisy time-series data of complex dynamical systems,” *Proceedings of the National Academy of Sciences*, vol. 121, no. 33, e2403771121, 2024. DOI: 10.1073/pnas.2403771121.

- [18] C. Lionello, M. Becchi, S. Martino, and G. M. Pavan, *Relevant, hidden, and frustrated information in high-dimensional analyses of complex dynamical systems with internal noise*, 2025. arXiv: 2412.09412 [physics.chem-ph].
- [19] S. Aghabozorgi, A. S. Shirkhorshidi, and T. Y. Wah, “Time-series clustering—a decade review,” *Information systems*, vol. 53, pp. 16–38, 2015. DOI: 10.1016/j.is.2015.04.007.
- [20] G. Palubinskas, X. Descombes, and F. Kruggel, “An unsupervised clustering method using the entropy minimization,” in *Proceedings. Fourteenth International Conference on Pattern Recognition (Cat. No. 98EX170)*, IEEE, vol. 2, 1998, pp. 1816–1818. DOI: <https://doi.org/10.1109/ICPR.1998.712082>.
- [21] A. P. Bartók, R. Kondor, and G. Csányi, “On representing chemical environments,” *Physical Review B—Condensed Matter and Materials Physics*, vol. 87, no. 18, p. 184 115, 2013. DOI: 10.1103/PhysRevB.87.184115.
- [22] C. Caruso, A. Cardellini, M. Crippa, D. Rapetti, and G. M. Pavan, “Timesoap: Tracking high-dimensional fluctuations in complex molecular systems via time variations of soap spectra,” *Journal of Chemical Physics*, vol. 158, no. 21, 2023. DOI: 10.1063/5.0147025.
- [23] M. Crippa, A. Cardellini, C. Caruso, and G. M. Pavan, “Detecting dynamic domains and local fluctuations in complex molecular systems via time-lapse neighbors shuffling,” *Proceedings of the National Academy of Sciences*, vol. 120, no. 30, e2300565120, 2023. DOI: 10.1073/pnas.2300565120.
- [24] C. E. Shannon, “A mathematical theory of communication,” *The Bell system technical journal*, vol. 27, no. 3, pp. 379–423, 1948. DOI: 10.1002/j.1538-7305.1948.tb01338.x.
- [25] E. S. Soofi, H. Zhao, and D. L. Nazareth, “Information measures,” *Wiley Interdisciplinary Reviews: Computational Statistics*, vol. 2, no. 1, pp. 75–86, 2010. DOI: 10.1002/wics.62.
- [26] S. M. Pincus, “Approximate entropy as a measure of system complexity,” *Proceedings of the national academy of sciences*, vol. 88, no. 6, pp. 2297–2301, 1991. DOI: 10.1073/pnas.88.6.2297.
- [27] J. S. Richman and J. R. Moorman, “Physiological time-series analysis using approximate entropy and sample entropy,” *American journal of physiology-heart and circulatory physiology*, vol. 278, no. 6, H2039–H2049, 2000. DOI: 10.1152/ajpheart.2000.278.6.H2039.
- [28] J. S. Richman, D. E. Lake, and J. R. Moorman, “Sample entropy,” in *Methods in enzymology*, vol. 384, Elsevier, 2004, pp. 172–184.
- [29] J. Abascal, E. Sanz, R. García Fernández, and C. Vega, “A potential model for the study of ices and amorphous water: Tip4p/ice,” *Journal of Chemical Physics*, vol. 122, p. 234 511, 2005. DOI: 10.1063/1.1931662.
- [30] E. D. Donkor, A. Laio, and A. Hassanali, “Do machine-learning atomic descriptors and order parameters tell the same story? the case of liquid water,” *Journal of Chemical Theory and Computation*, vol. 19, no. 14, pp. 4596–4605, 2023. DOI: 10.1021/acs.jctc.2c01205.
- [31] S. Martino, D. Doria, C. Lionello, M. Becchi, and G. M. Pavan, *A data driven approach to classify descriptors based on their efficiency in translating noisy trajectories into physically-relevant information*, 2024. arXiv: 2411.12570 [cond-mat.mtrl-sci].
- [32] E. D. Donkor, A. Offei-Danso, A. Rodriguez, F. Sciortino, and A. Hassanali, “Beyond local structures in critical supercooled water through unsupervised learning,” *Journal of Physical Chemistry Letters*, vol. 15, no. 15, pp. 3996–4005, 2024. DOI: 10.1021/acs.jpclett.4c00383.
- [33] C. R. Schwantes and V. S. Pande, “Modeling molecular kinetics with tica and the kernel trick,” *Journal of chemical theory and computation*, vol. 11, no. 2, pp. 600–608, 2015. DOI: 10.1021/ct5007357.
- [34] M. Hoffmann, M. K. Scherer, T. Hempel, *et al.*, “Deeptime: A python library for machine learning dynamical models from time series data,” *Machine Learning: Science and Technology*, 2021. DOI: 10.1088/2632-2153/ac3de0.
- [35] O. A. Karim and A. Haymet, “The ice/water interface: A molecular dynamics simulation study,” *Journal of Chemical Physics*, vol. 89, no. 11, pp. 6889–6896, 1988. DOI: 10.1063/1.455363.
- [36] I. Assent, “Clustering high dimensional data,” *Wiley Interdisciplinary Reviews: Data Mining and Knowledge Discovery*, vol. 2, no. 4, pp. 340–350, 2012. DOI: 10.1002/widm.1062.
- [37] N. Kouroukidis and G. Evangelidis, “The effects of dimensionality curse in high dimensional knn search,” in *2011 15th panhellenic conference on informatics*, IEEE, 2011, pp. 41–45. DOI: 10.1109/PCI.2011.45.
- [38] N. Altman and M. Krzywinski, “The curse (s) of dimensionality,” *Nat Methods*, vol. 15, no. 6, pp. 399–400, 2018. DOI: 10.1038/s41592-018-0019-x.
- [39] M. Becchi and G. M. Pavan, *Research data supporting: “maximum information extraction from noisy data via shannon entropy minimization”*, Apr. 2025. DOI: 10.5281/zenodo.15236524.
- [40] GMPavanLab, *Dynsight: A framework for the analysis of the dynamics of particle trajectories*, <https://github.com/GMPavanLab/dynsight>, Accessed: 31-03-2025, 2023.

Supplemental Material for “Maximum Information Extraction via Data clustering and Shannon Entropy Minimization”

Matteo Becchi, Giovanni M. Pavan

Supporting Figures

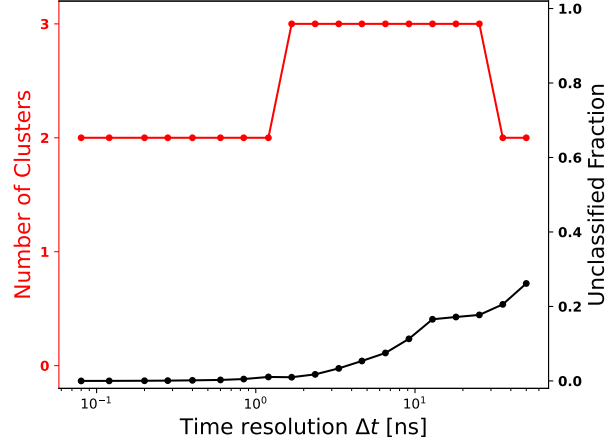


Figure S1: Number of cluster discovered (red) and fraction of unclassified data points (black) as a function of the time resolution Δt used for the onion clustering on SOAP PC1 data.

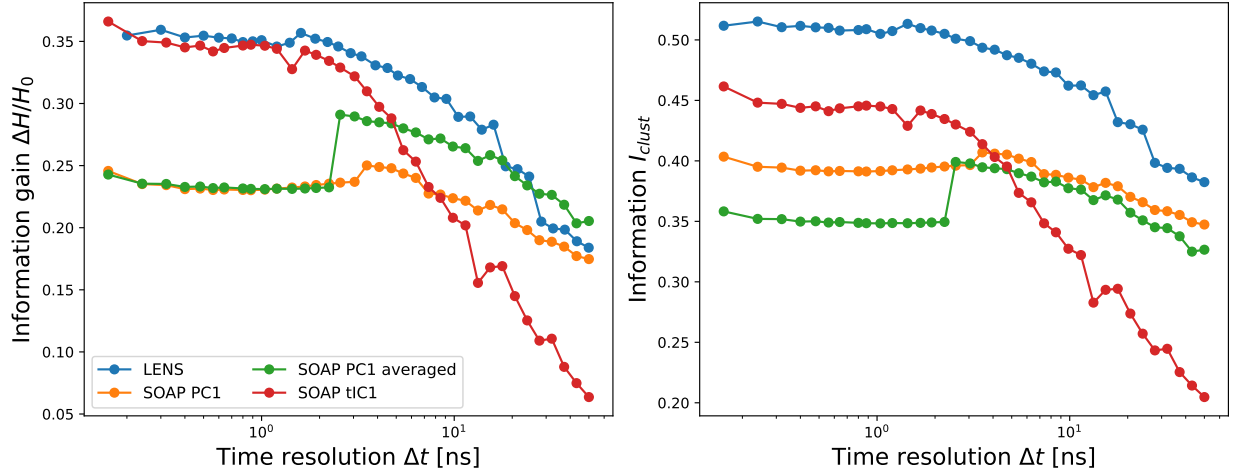


Figure S2: Comparison between different descriptors. Relative information gain $\Delta H/H_0$ (on the left) and information after clustering I_{clust} (on the right) for different single-particle descriptors. In blue, LENS (mentioned in the main text), smoothed with a Butterworth low-pass filter. In orange, the first Principal Component (PC1) of SOAP, and in green the same quantity smoothed using spatial average (see main text). Finally, the red curve is the first time-delay Independent Component (tIC1) obtained using the algorithm presented in [33], [34].

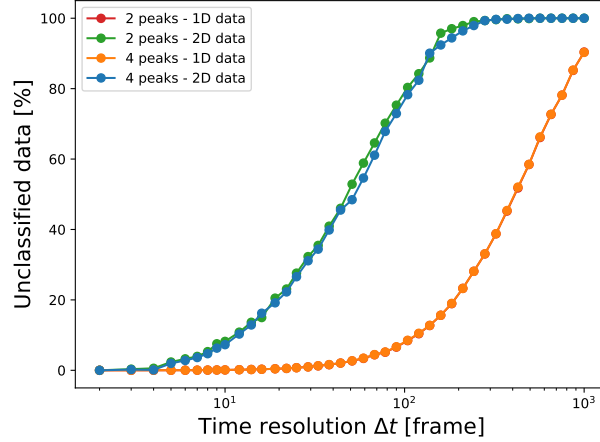


Figure S3: The fraction of unclassified data points in the four Langevin dynamics datasets. As can be seen, by clustering bi-dimensional datasets (blue and green curves) this fraction grows faster with Δt . Color coding is consistent with Fig. 3. Notice that the red and orange curves are tightly superimposed.

Simulation details

Ice/liquid water coexistence

An initial configuration for the system is obtained combining configurations of liquid water and I_h ice, each one containing 1024 TIP4P/ICE molecules [29]. This system was equilibrated for 10 ns at ambient pressure and temperature $T = 268$ K. Finally, the production run was performed in NPT conditions, at the same temperature and pressure, for 50 ns, with a sampling time interval of $\delta t = 0.04$ ns. The simulation follows the same protocol illustrated in detail in Ref. [22].

SOAP power spectra calculation

At every trajectory frame t along the TIP4P/ICE MD trajectories, we computed the SOAP power spectrum for each molecule using the parameters $n_{\max} = n'_{\max} = l_{\max} = 8$ and a cutoff radius $r_c = 10$ Å. Each SOAP spectrum consists of 576 components. To reduce dimensionality, we performed Principal Component Analysis (PCA), keeping only the first PC for the following analyses. Signals were then denoised using the protocol reported in Ref. [32].

Bi-dimensional Langevin dynamics

The Langevin dynamics (in the limit of zero friction)

$$x(t + \delta t) = x(t) + \sqrt{2D\delta t} \cdot \eta(t) \quad (\text{S1})$$

of 100 particles moving in a bi-dimensional plane was simulated using in-house Python code, for $1e5$ time-steps, with a time increment $\delta t = 0.01$ and a diffusion coefficient $D = 0.6$, with $\eta(t)$ random Gaussian noise. The free energy landscapes have two and four minima, located in $(0, 0)$, $(0, 1)$ and $(0, 0)$, $(0, 1)$, $(1, 0)$, $(1, 1)$ respectively, and are defined as

$$U(x, y) = -\ln \left[\exp \left(-\frac{x^2 + y^2}{2\sigma^2} \right) + \exp \left(-\frac{x^2 + (y-1)^2}{2\sigma^2} \right) \right] \quad (\text{S2})$$

(and analogously for the 4 minima version, and for the three-dimensional version) with $\sigma = 0.12$.

Methods details

Static dataset clustering

The results shown in Fig. 1d are obtained using onion clustering with $\Delta t = \tau = 50$ ns, thus clustering time-series as belonging on one of the two main environments (ice, in blue, and liquid, in orange) or unclassified (in gray). Similar results can be obtained using any Gaussian Mixture Model with $k = 2$ components on the flattened dataset.

Shannon entropy calculations

Given a dataset of measured values $\{x_i\}$, with $i \in \{0, \dots, N - 1\}$, we construct a histogram $\{b_j, p_j\}$, where b_j are the bins and p_j are the normalized counts ($\sum_j p_j = 1$). Notice that to build the histogram, the number of bins n_b has to be chosen. The Shannon entropy of the dataset is then

$$H = - \sum_{j=0}^{n_b} p_j \log_2 p_j \quad (\text{S3})$$

After the data are clustered with a suitable algorithm, obtaining K clusters, each containing values $\{x_i\}_k$, the same procedure is applied to compute each cluster's entropy H_k , using the same binning $\{b_j\}$ as for the full dataset. Using Eqs. 2 and 3, we can then compute the information gain as

$$\Delta H = H - \sum_{k=1}^K f_k H_k \quad (\text{S4})$$

Notice that in a trivial clustering where all data points belong to a single cluster, $\Delta H = 0$, as expected. Similarly, for a random clustering that distributes points into K clusters with identical distributions, the information gain vanishes on average. Throughout the text, all Shannon entropy are normalized between 0 and 1 by dividing them by the maximum possible entropy, $\log_2 n_b$. A number of bin $n_b = 20$ was used; different number of bins, up to $n_b = 40$, were tested, giving qualitatively comparable results. All the code used to perform the analyses for this work is based on the Dynsight software [40].